

Revista Politécnica

ISSN: 1900-2351 ISSN: 2256-5353

rpolitecnica@elpoli.edu.co

Politécnico Colombiano Jaime Isaza Cadavid

Colombia

Ospina Alarcón, Manuel Alejandro; Usuga Manco, Liliana María EFECTO DE LAS FUERZAS HIDRODINÁMICAS SOBRE LA TRAYECTORIA DE PARTÍCULAS MINERALES EN CONCENTRADORES GRAVIMÉTRICOS TIPO JIG

> Revista Politécnica, vol. 14, núm. 27, 2018, Julio-, pp. 68-79 Politécnico Colombiano Jaime Isaza Cadavid Colombia

DOI: https://doi.org/doi.org/10.33571/rpolitec.v14n27a7

Disponible en: https://www.redalyc.org/articulo.oa?id=607866319008





Más información del artículo

Página de la revista en redalyc.org



Sistema de Información Científica Redalyc

Red de Revistas Científicas de América Latina y el Caribe, España y Portugal Proyecto académico sin fines de lucro, desarrollado bajo la iniciativa de acceso

abierto

EFECTO DE LAS FUERZAS HIDRODINÁMICAS SOBRE LA TRAYECTORIA DE PARTÍCULAS MINERALES EN CONCENTRADORES GRAVIMÉTRICOS TIPO JIG

Manuel Alejandro Ospina Alarcón¹, Liliana María Usuga Manco²

¹PhD en Ingeniería: Ciencia y Tecnología de Materiales. Docente Instituto Tecnológico Metropolitano.Grupo de investigación AEyCC.Medellín-Colombia. manuelospina@itm.edu.co

²PhD en Ingeniería: Ciencia y Tecnología de Materiales.Docente Instituto Tecnológico Metropolitano. Medellín-Colombia. lilianausuga8168@correo.itm.edu.co

RESUMEN

La interacción hidrodinámica es un proceso sensible para los equipos de concentración gravimétrica. Debido a la no linealidad y complejidad de la interacción dinámica de las partículas sólidas y el aqua, se necesitan modelos matemáticos confiables para desarrollar tareas de diseño total de planta (DTP). Para este fin, en este artículo se presenta un estudio del movimiento de partículas sometidas a un flujo pulsante para un perfil sinusoidal de agua en un jig, el cual es un equipo de concentración gravimétrica de alto rendimiento y alta recuperación, ampliamente utilizado en el procesamiento de minerales. Se utiliza el modelo matemático Euleriano-Lagrangiano (ELM), donde el movimiento del fluido se calcula mediante solución de las ecuaciones de Navier-Stokes y continuidad por medio de un procedimiento numérico ampliamente usado. Ilamado método semi-implicito para resolver las ecuaciones asociadas a la presión (SIMPLE). El movimiento individual de las partículas se obtiene por medio de un balance de fuerzas aplicando la segunda ley de movimiento de Newton a través de la acción de las fuerzas impuestas por el fluido y la gravedad. Las fuerzas de interacción sólidolíquido se calculan mediante el modelo matemático, extendido a una suspensión de partículas que poseen distribución amplia de tamaño y densidad. Los cálculos y la comparación de las fuerzas de Basset, gradiente de presión y masa virtual con las otras fuerzas (arrastre y empuje) que actúan sobre la trayectoria de las partículas en flujo de agua oscilatorio se llevaron a cabo para régimen de flujo turbulento. Se encontró que las fuerzas de Basset, gradiente de presión y masa virtual tienen un efecto significativo sobre la trayectoria de las partículas que ingresan al jig, influenciando su posterior concentración. Además, se determinaron, las condiciones bajo las cuales estas fuerzas pueden despreciarse en el modelo hidrodinámico del jig. El estudio mostró diferencias significativas en la trayectoria de las partículas para diferentes distribuciones de tamaño y densidad.

Palabras clave: Interacción sólido-líquido, Concentración gravimétrica, Simulación numérica, Suspensiones de alta densidad, Modelo Euleriano-Lagrangiano

Recibido:14 de septiembre de 2018. Aceptado:20 de noviembre de 2018 Received: September14th, 2018. Accepted: November 20th, 2018

EFFECT OF HYDRODYNAMIC FORCES ON MINERAL PARTICLES TRAJECTORIES IN GRAVIMETRIC CONCENTRATOR TYPE JIG

ABSTRACT

Hydrodynamic interaction is a sensitive process for gravity concentration equipment. Because of the nonlinearity and complexity of interaction dynamics due the solid particles and water, reliable mathematical models are needed to perform plant width design (PWD)-oriented tasks. To this end, in this paper we present a study of particle motion in a water oscillating flow subjected to a sinusoidal profile on a jig device, which is a high yield and high recovery gravimetric concentrator device widely used in minerals processing. A mathematical Eulerian-Lagrangian model (ELM) is used where fluid motion is calculated by solving the Navier-Stokes and continuity equations by a widely used numerical procedure call Semi-Implicit Method for Pressure Linked Equations algorithm (SIMPLE). The motion of individual particles is obtained by a forces balance applying the Newton's second law of motion through the action of forces imposed by the water and gravity. Liquid-solid interactions forces are calculated by the mathematical Eulerian-Lagrangian model extended to a particle suspension having a wide size and density distribution. The calculation and comparison of Basset, pressure gradient and virtual mass forces with other forces (drag and buoyancy) acting on particle trajectories in water oscillating flows were carried out under turbulent regimen flow. It was found that Basset, pressure gradient and virtual mass forces have a significant effect on the particle's trajectories affecting their subsequent stratification. Furthermore, the conditions under which these forces can be neglected in the jig's hydrodynamic model were studied. The study demonstrates significant differences in the particle trajectories for various size and density distribution.

Keywords: Solid-liquid interaction, Gravimetric concentration, Numerical simulation, High density suspensions, Eulerian-Lagrangian model.

Cómo citar este artículo: M. A. Ospina Alarcón, L. M. Usuga Manco, "Efecto de las fuerzashidrodinámicas sobre la trayectoria de partículas minerales en concentradores gravimétricos tipo JIG", Revista Politécnica, vol. 14, no. 27 pp.68-79, 2018. https://doi.org/10.33571/rpolitec.v14n27a7

1. INTRODUCTION

Gravity concentration describes the gradual removal of heavy minerals from the ganga through mechanical processes for industrial Typically, a gravity concentration plant (GCP) includes a primary treatment (physical separation) and a secondary treatment to recover the valuable mineral [1]. Primary treatment consists of a chain of gravity concentration devices as a Jig (see Fig. 1. [1]) where mineral particles move relatively in a pulsating water flow resulting in a stratification of particles of different densities and sizes [2]. Due to the ever increasingly stringent requirements imposed by mining legislation [3], control of effluent standards requires refined and sophisticated process design able to minimizing environmental contamination to water sources.

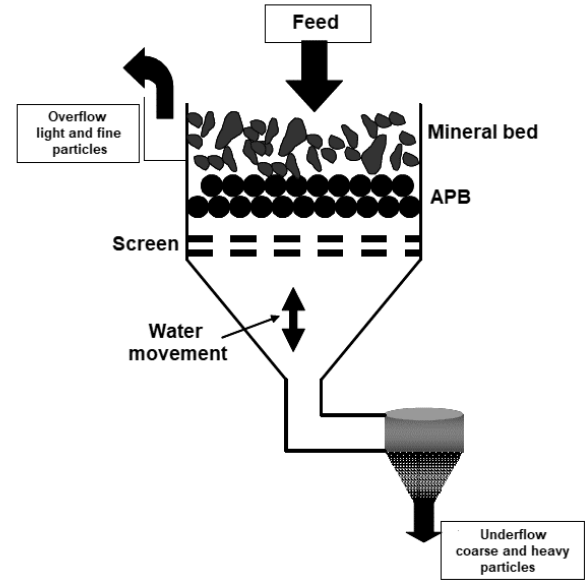


Fig. 1.Basic jig outline [1].

One of the most important stages in a GCP is related to recovery equipments [4]. In a GCP, the recovery stage is responsible for two main task, namely, particle separation by density and hindered settling, and raise the content of the concentrated mineral in the underflow [5]. The former is needed to particles stratification inside de jig, that happen in a turbulent multiphase flow system (pulsating flow, solid-liquid and solid-solid interactions) [4]. In this regard, when the particles are exposed to different water wave formsas sinusoidal, sawtooth and trapezoidal (water velocity field), different operating variables will affect the trajectories of particles.

They include feed water rate, amplitude and frequency of oscillating flow, etc. [6], [7]

When oscillating flow reach low amplitude levels of water velocity (ui<0.001 m/s), undesired concentration occurs [6], [7]. On the other hand, high amplitude levels of water velocity (ui>0.01 m/s) contribute to the acceleration of mineral particles and may inhibit the particle settling. Therefore, variation in the oscillating flow affect the jig performance, the degree of treatment, and finally, the mineral recovery in the underflow. In addition, according to Dong et al. [8], particle separation is an energy intensive process within a GCP. In fact, it is estimated that around 50-75% of the GCP power consumption is due to gravity particle separation [8].

From the dynamical point of view, a GCP can be classified as a complex system with multivariable nonlinear dynamics, large uncertainty according to external disturbances and both model structure and parameters, and multiple space and time scales dynamics [9]. Therefore, controlling recovery in the concentrate stream (under flow) in Jigs is, in general, not a straightforward task. These issues motivated the study of dynamic behavior of GCPs by means of modeling and simulation tools. As pointed out by Dong et al. [8], There are several benefits to modeling GCPs: plant design and optimization, experimental design, testing research hypotheses, design and evaluation of control strategies, forecasting, analysis of plant-wide performance, and education [7], [8].

For design and optimization purposes of GCPs, the PET (potential energy theory) [10], [11]and DEM (discrete element method) [12]-[19]simulation models are widely used to try understand the gravimetric concentration process in jigs. For instance, in Mayer [10] experimental configurations in jigging processes are derived from optimal recovery profiles meeting a change of water strokes. In Tavares and King [11], novel strategies for Mayer's theory are derived and applied to a Jig by using a formal modeling methodology accounting for a phenomenological description of the particle stratification. However, the above contributions don't address the recovery to the concentration of minerals particles widely distributed in size and density. Therefore, the investigations of Ospina and Bustamante [20] and Ospina [21] were the starting point.

Over the years, DEM models with a more detailed description of the gravity particle separation phenomenon are being used more often in order to obtain a quantitative analysis of concentration process in jig [9]. However, in spite of that progress, some challenges remain. For instance, one of the main goals that has not been accomplished so far is an agreed mathematical description of the hvdrodvnamics interaction. Roughly speaking. represents hydrodynamics interaction the resistance to performing the gravity particle separation by density and size from the liquid (medium) through a specific pulse wave (amplitude and frequency) to the solid (mineral particles). The hydrodynamics interaction turns out to be of paramount importance since it is directly related to the particle concentration.

Currently, the literature provides different ways to determine the hydrodynamics interaction inside the jig chamber, Mishra and Mehrotra [17], Beck and Holtham [19], Srinivasan et al. [16] and Mishra and Mehrotra [18], use a DEM models by incorporating constant or lineal approximation for hydrodynamics forces or take on a uniform fluid field and did not consider the effect of possible non-uniform fluid velocity on particle hydrodynamic forces. Also, assume the stratification as a batch process and neglected forces such as Basset history, virtual mass and pressure gradient without showing a preliminary analysis of their importance when calculating the trajectories that followed the particles that entering to jig separation chamber. In spite of the many available ways to determine the hydrodynamics interaction in Jigs vessels, the main observed concern about the above approaches is that they are only useful in the systems from which they were developed [12]-[15].

This paper aims to use a mathematical model to study and simulate the particle trajectories fed to jig and its interaction with other internal process variables. First an Eulerian-Lagrangian model (ELM) is obtained to describe the dynamic behavior of Jig. Then, the different available approximations of the hydrodynamics forces are tested and assessed in terms of their ability to describe the interaction phenomenon in the jig.

The work is organized as follows. Section 2 presents an overview of Eulerian-Lagrangian model and main settings for understand the interaction phenomenon in a jig concentrator. Then, in Section 3, the simulation procedure is followed for the

process of interest to obtain a dynamical model of the jig. In Section 4, the reviewed approximations are compared and assessed by using them as the hydrodynamic forces analysis for the hydrodynamic interaction in the developed model. Finally, Section 5 gives the main conclusions and ideas for future research.

2. EULER LAGRANGE MODEL DESCRIPTION

The Euler-Lagrange model (ELM) have a wide use in present-day engineering [3], [7], [21]-[25]. In this contribution, special attention is paid to calculate the water flow in an Euler coordinates where the particles are moved individually in Lagrangian frame. As is well known, mineral and metallurgical processing models are complex and nonlinear due to the multiple interacting phenomena (solid - liquid interaction), making them hard to implement in plant width design (PWD)-oriented tasks. An ELM (a type of distributed parameters model) is able to capture the essential phenomena (mass, energy, and momentum transfer) giving an important insight into the process, thus providing strategies to rationally design and optimize industrial scale concentrators. An ELM may help to understand the phenomena that occur inside the industrial gravity concentrator, contributing to the process development.

ELMs have the following properties [3], [7], [21]–[25]:

- Uniqueness in structure: it means that model structure comes from phenomenology, especially, conservation laws (balanceequations).
- Modular structure: ELM can grow from its simplest model, including more variables or phenomena. It also applies to model parameters represented as ELM sub-models.
- Combination of levels of detail: it might provide a framework for a more accurate model response, sharing multiple levels, from macroscopic to molecular/atomic scales.
- Model interpretability: ELMs may be built up such that the physical meaning of the model parameters is conserved, easing the parameters identification.

The Euler-Lagrangian jig model is based on CFD techniques and is particularly suitable for studying particle behavior in the turbulent flows. The water is considered as a continuous phase, and the solid particles are accounted for a dispersed phase. The model calculates the solid-liquid interactions time dependent on the concentration process in the jig solving the Unsteady Reynolds averaged Navier-

Stokes equations (URANS) with the standard turbulence model k- ϵ [26].

A modeling methodology for ELMs has been evolving for many years [11], [14], [16], [18], [27]–[32]. This methodology is built upon the seminal work of Beck and Holtham (1993) [19] and Mishra and Mehrotra (1998) [17] and described by steps detailed in Viduka*et al.* (2013) [9] and Ospina and Bustamante [20].

2.1. Liquid phase hydrodynamics

The water velocity field is calculated by solving the dynamic conservation equations. Since no mass exchanges or chemical reactions are considered between water and minerals particles in the proposed model, the continuity equation of water can be formulated without the exchange term as shows in Eq. (1):

$$\frac{\partial}{\partial t}(\rho_l \phi_l) + \frac{\partial}{\partial x_i}(\rho_l \phi_l u_i) = 0 \tag{1}$$

The momentum balance for the water in multiphase flow is described in following general formulation as described in Eqs. (2) and (3):

$$\begin{split} \frac{\partial}{\partial t} (\rho_{l} \phi_{l} u_{i}) + \frac{\partial}{\partial x_{i}} (\rho_{l} \phi_{l} u_{i} u_{j}) &= \cdots \\ \cdots - \frac{\partial P}{\partial x_{i}} + \frac{\partial}{\partial x_{j}} \Gamma \left(\frac{\partial u_{i}}{\partial x_{j}} + \frac{\partial u_{j}}{\partial x_{i}} \right) \cdots \\ \cdots + \rho_{l} \phi_{l} g_{i} + F_{wi} \\ \Gamma &= \mu + \mu_{t} \end{split} \tag{2}$$

where $\phi_i,~\rho_i$ and u_i are the water volume fraction in a computation cell, water density and water velocity component, respectively. P is the pressure, F_{wi} is momentum transfer term, g_i is the gravity acceleration and Γ is the viscosity composed of water viscosity μ and turbulent viscosity $\mu_t.$ The subscripts i and j represents coordinate axes directions. The k- ϵ model can be incorporated into the program to calculated water turbulent viscosity.

2.2. Particle motion equation

For a particulate system with a size distribution (from 125 μ m to 2000 μ m) and density distribution (from 3000 kg/m³ to 13800 kg/m³), the description of the particle trajectories and interaction between the particles and water depends on the correct calculation of the hydrodynamic forces involved. It is assumed that the forces acting on a solid spherical particle moving in a dynamic and non-uniform water flow field are composed of separate and uncoupled contributions from the water drag force, the pressure gradient force, virtual mass force, Basset history force [33] and the gravitational body force [8]. The Lagrangian equation of particle motion can be written in this approximation as shows in Eq. (4).

$$\begin{split} m_p \frac{d\mathbf{u}_p}{dt} &= \cdots \\ \cdots - \frac{\pi}{8} C_d \rho_l d_p^2 \Big| \mathbf{u}_p - \mathbf{u}_l \Big| \Big(\mathbf{u}_p - \mathbf{u}_l \Big) \cdots \\ \cdots - \frac{1}{2} \rho_l V_p \Big(\frac{d\mathbf{u}_p}{dt} - \frac{D\mathbf{u}_l}{Dt} \Big) \cdots \\ \cdots - \rho_l V_p \frac{d\mathbf{u}_l}{dt} \cdots \\ \cdots - \rho_l V_p \frac{d\mathbf{u}_l}{dt} \cdots \\ \cdots + \Big(\rho_p - \rho_l \Big) V_p \mathbf{g} \end{split} \tag{4}$$

The five terms on the right-hand side of Eq. (4) are, in order from left to right, drag force, virtual mass force, pressure gradient force, Basset history force and buoyancy force, respectively. Where m_p , V_p , d_p , p_p are the mass, the volume, the diameter and the density of the particle, respectively, \mathbf{u}_p , \mathbf{u}_l are particle and water velocities respectively and C_d is the drag coefficient, which for a spherical particle is a function of particle Reynolds numbers, expressed by Schiller and Naumann [34] correlation in the flow regime considered.

The calculation of particle trajectories requires the solution of two ordinary differential equations, one for the calculation of the velocity (\mathbf{u}_p) and one for the calculation of the position (\mathbf{x}_p) that in their vector form are expressed in Eqs. (5) and (6):

$$m_{p_i} \frac{d\mathbf{u}_p}{dt} = \sum \mathbf{f}_i \tag{5}$$

$$\frac{d\mathbf{x}_{p}}{dt} = \mathbf{u}_{p} \tag{6}$$

where f_i represents the different relevant forces acting on a particle due to the viscous interaction

with the water. The trajectories of particles can be obtained by numerical integration of Eqs. (5) and (6). The instantaneous water velocity components at the particle location required for calculation of forces in Eq. (4) are determined from the local mean water velocity interpolated from the neighboring Euler grid points using area weighted averaging techniques.

3. SIMULATION PROCEDURE

3.1. Importance of the different forces

Navier–Stokes equation (2) is solved by the "SIMPLE" (Semi-Implicit Method for Pressure Linked Equations) method in a 2D domain [35]. In this method, the partial differential equations for the mass and the momentum are solved by integrating the differential equations (1) and (2) over control volumes. For this, an orthogonal grid is applied (60x100 grids) where two velocities and pressures are stored in the staggered positions.

The linearization of the non-linear equations is performed by a "hybrid" difference method to get an implicit finite difference scheme. In this scheme, at a high Peclet number (Pe), it switches from central to upwind differencing for convection terms; for diffusion terms, the central differencing is used constantly. Due to the elliptic nature of the partial equations, iterative differential an procedure is employed. Starting with guessed distributions for the velocity and pressure fields, the fluid velocities can be calculated from the momentum equation (2). Further, the pressure correction equation which has been derived from the continuity equation (1) is used to yield the corrected values for the velocity and the pressure fields so that the continuity equation is implicitly satisfied. With the corrected values, the momentum equations are solved again and the whole procedure is repeated until convergence achieved [36] and [31].

3.2. Solving of particle motion equation by Runge-Kutta method

Calculation of the particle trajectories by solving the equation of motion of the particles, as well as the calculation of the particle source terms, is performed in the same iteration loop after the solution of the water flow equations, to handle the iteration between the fluid and the particles. The change in particle velocity is calculated by

integrating the equations (5) and (6) via a fourthorder Runge–Kutta method at each time instant updating the position of particles after the interaction with the water. [18].

3.3. Boundary conditions

The particle movement and water velocity field are simulated in a 2-D column with height of 0.1 m and width 0.05 m. The following assumptions were made regarding boundary conditions in this simulation:

At the chamber jig walls, water has non-slip conditions.

The water inlet velocity at bottom of the column can be specified.

The inlet water flow enters chamber from center of the bottom.

The axial liquid velocity gradient at the bottom and the top is zero.

Finally, the model was simulated in two software applications, MATLAB®9.2(R2017a) and ANSYS Fluent 12.1 using anuser define function (UDF)to couple the water velocity field and the RungeKutta method to calculate the particle trajectories, these programs were installed in a computer with an 4-core processor and 8GB of RAM. We used a sampling time $t_{\rm s}=0.01~\rm s.$

4. HYDRODYNAMIC FORCES ANALYSIS

The motion equation of particles is obtained from Newton's second law of motion (4). The forces driving significantly the particle motion are: the force corresponding to buoyancy that is expressed by Eq. (7) and the viscous drag force of flow that passes through the particle that is given by Eq. (8).

$$\mathbf{F}_{g} = (\rho_{p} - \rho_{l}) V_{p} \mathbf{g} \tag{7}$$

$$\mathbf{F}_{\mathrm{D}} = \frac{\pi}{8} C_{\mathrm{d}} \rho_{\mathrm{I}} d_{\mathrm{p}}^{2} \left| \mathbf{u}_{\mathrm{p}} - \mathbf{u}_{\mathrm{I}} \right| \left(\mathbf{u}_{\mathrm{p}} - \mathbf{u}_{\mathrm{I}} \right)$$
 (8)

When the drag force obtained in (8) is balanced with the buoyancy force in (7), the terminal velocity in Stokes regime, u_s , of particle is obtained as in the Eq. (9) [37]:

$$u_s = \frac{d_p^2 \Delta \rho g}{18\mu_1} \tag{9}$$

It is important to note that neglecting the transient part of the inertia does not imply that the flow is

steady. It means that the forces on the water are in dynamical equilibrium, this equilibrium happening in a time-scale much shorter than the time in which the particle motion is developed. Therefore, the instantaneous structure of the flow depends on the boundary conditions of the phenomenon only. In this case, the flow (and the force acting on the particle) is said to be quasi-steady [30].

The unsteady forces \mathbf{F}_{MV} and \mathbf{F}_{VP} are associated to the inertia and the acceleration of the fluid surrounding the particles. They are called the virtual mass force and pressure gradient force respectively and can be calculated from the potential flow passing through particles[38], namely Eqs. (10) and (11):

$$\mathbf{F}_{MV} = \frac{1}{2} \rho_{I} V_{p} \left(\frac{d\mathbf{u}_{p}}{dt} - \frac{D\mathbf{u}_{I}}{Dt} \right)$$
 (10)

$$F_{\nabla P} = \rho_I V_p \frac{d\mathbf{u}_I}{dt} \tag{11}$$

Note that the coefficient of the time derivative in Eq. (10) is the mass of fluid associated with half of the volume of the particle, corresponding to the mass of fluid accelerated by the particle.

The expression for the Basse force \mathbf{F}_B is given by the following convolution integral in Eq. (12) [19].

$$\mathbf{F}_{B} = \frac{3}{2} d_{p}^{2} \sqrt{\pi \mu_{l} \rho_{l}} \int_{0}^{t} \frac{\left(\frac{d\mathbf{u}_{p}}{dt} - \frac{D\mathbf{u}_{l}}{Dt}\right)}{\sqrt{t - \tau}} d\tau \tag{12}$$

where τ is an integration variable. This force couples the history of the acceleration of the particle with the viscosity of the water, indicating a transient diffusion of vorticity in the flow [30].

Now, we consider the 1-D version of Eq. (4) adopting the positive sense of motion downwards. By this convention, the drag forces that resist the motion of the particle are negative forces. Is then obtained the Eq. (13):

$$\begin{split} m_p \frac{du_p}{dt} &= \cdots \\ \cdots - \frac{\pi}{8} C_d \rho_l d_p^2 \Big| u_p - u_l \Big| \Big(u_p - u_l \Big) \cdots \\ \cdots - \frac{1}{2} \rho_l V_p \Bigg(\frac{du_p}{dt} - \frac{Du_l}{Dt} \Bigg) \cdots \\ \cdots - \rho_l V_p \frac{du_l}{dt} \cdots \end{split} \tag{13}$$

$$\begin{split} \cdots - & \frac{3}{2} d_p^2 \sqrt{\pi \mu_I \rho_I} \int\limits_0^t \! \frac{\left(\frac{du_p}{dt} - \! \frac{Du_I}{Dt} \right)}{\sqrt{t - \tau}} \! \! d\tau \cdots \\ & \cdots + \left(\! \rho_p - \! \rho_I \right) \! V_p g \end{split}$$

where u_p y u_l are the dimensional 1-D particle velocity and water respectively and ${\rm g}$ is the acceleration of gravity.

Eq. (13) can be made nondimensional by choosing the terminal Stokes velocity u_s in Eq. (9) and the particle relaxation time τ_r in Eq. (14) as the characteristic velocity and time scales, respectively.

$$\tau_{r} = \frac{d_{p}^{2} \rho_{p}}{18\mu_{1}} \tag{14}$$

Defining the dimensionless variables: \bar{u}_p in Eq.(15), \bar{u}_l in Eq. (16) and \bar{t} in Eq. (17), organizing and grouping terms, the Eq. (13) can be written in a nondimensional form by Eq. (18).

$$\hat{u}_p = \frac{u_p}{u_s} \tag{15}$$

$$\widehat{u}_{l} = \frac{\mathsf{u}_{l}}{\mathsf{u}_{s}} \tag{16}$$

$$\hat{t} = \frac{t}{\tau_r} \tag{17}$$

$$\left(1 + \frac{1}{2}\chi\right) \frac{d\hat{u}_{p}}{d\hat{t}} = \cdots$$

$$\cdots - \frac{C_{d}Re_{s}}{24} |\hat{u}_{p} - \hat{u}_{l}| (\hat{u}_{p} - \hat{u}_{l}) \cdots$$

$$\cdots + \frac{1}{2}\chi \frac{D\hat{u}_{l}}{D\hat{t}} - \chi \frac{d\hat{u}_{l}}{d\hat{t}} \cdots$$

$$\cdots - \sqrt{\frac{9}{2\pi}\chi} \int_{0}^{\tau_{r}\hat{t}} \left(\frac{d\hat{u}_{p}}{d\hat{t}} - \frac{D\hat{u}_{l}}{D\hat{t}}\right) \frac{d\zeta}{\sqrt{\hat{t} - \zeta}} + 1$$
(18)

In Eq. (18), three relevant physical parameters governing the particle motion, are identified: the density ratio ($^{\chi=\rho_l/\rho_p}$), the drag coefficient (C_d) and the Reynolds number based on the Stokes terminal velocity ($^{\mbox{Re}_s=\rho_l d_p u_s/\mu_l}$). It should be noted that if the terminal velocity of the particle uthad been chosen as a velocity scale, instead of us, we would find, in addition to the Reynolds

number and the density ratio, the sedimentation number $N_s = u_s/u_t$ (note that for the Stokes regime, $u_t = u_s$ and $N_s = 1$). Eq. (18) is an integrodifferential nonlinear first-order differential equation and is associated to the initial condition $\hat{u}_p(0) = \hat{u}_0$ and an analytical solution of Eq. (18) in its complete form has not yet been obtained [10].

It is appropriate name the terms related to the accelerations (second, third and fourth term on the right-hand side of Eq. (18)), inertial forces. The inertial forces are assumed to be small and have been neglected in most of the studies related to particles movement and stratification in jigs, i.e. only one study, knowledge of the authors available in the literature that provides a general analysis of the effect of the inertial forces on the stratification, velocities and trajectories of the particles in the jig. Asakuraet al. [27] was the only study that mentioned the inclusion of the Basset force for the trajectory and the dynamic response time of a single particle in a jig.

The significance of inertial terms especially the Basset force is not easy to determine [28]. However, the inertial terms may be neglected for

density relations $\rho_I/\rho_p \ll 1$ such as those systems are composed of particles moving in gases, where the particle density is much greater than the gas density. Steady state movement and the terminal velocity is not affected by this term, however, when the motion equation (18) is analyzed, it is observed that all inertial terms have density ration χ as parameter, it being necessary include in the final trajectory analysis. Not include water acceleration terms can lead to erroneous and physically unacceptable results, that is, in particulate systems in which particle density is of the same magnitude order that fluid density (as is the jig case), the χ term dominates the particles trajectory (see Fig. 2).

Fig. 2 display vertical displacement of a particle whit size d=300 μ m and relative density RD= 3.562 under a sinusoidal pulsation profile and shows that the motion is significantly affected by the inclusion of virtual mass force (F_{VM}) and Basset force (F_B). Therefore, from Fig. 2 it is observed that with respect to F_B the particle trajectory varies significantly. When only is taken into account buoyancy force (F_D) and drag force (F_D) on motion equation (4), it is not to be expected that the particles are reported in the underflow, but with the

inclusion of inertial forces, particles actually concentrate under the amplitude and frequency adjusted. Do not include the water effect leads to an infinitely large initial acceleration which is physically unacceptable [39] and [40].

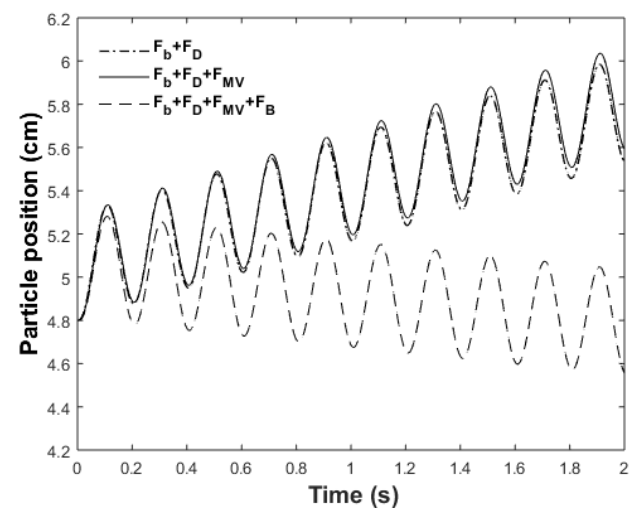


Fig. 2. Vertical movement of particles including Basset force (F_B) and virtual mass force (F_{MV}). Source: Authors.

5. RESULTS AND DISCUSSION

5.1. Importance of the different forces

Analysis of the importance of the different hydrodynamic forces acting on a particle in jigging is performed for different sized particles and for particles with different densities with pulsation water flow. The results of these analysis are shown in Fig. 3 and Fig. 4.

In Fig. 3 particles have a uniform size of d=300 μ m but with a relative density composition range from 3 to 13.8. The fluidizing water velocity is 5.841 cm/s and solid concentration is about 6% at an instant time t = 5 s. It was shown that the drag force and buoyancy force are dominant forces and they have a nearly linear relationship with particle densities. Virtual mass force has the smallest magnitude order among all forces. Basset force is about one order smaller than drag force.

The relative magnitudes of different forces are compared in Fig. 4 for all particles with a constant relative density value of RD=3.42 and keep other parameters constant. The size range is 125 μ m to 2000 μ m. As shown in Fig. 4, the drag force and

buoyancy force are still the dominant forces with an exponential relationship with size. However, it should be noted that Basset, added mass and pressure gradient might increase to about 10% of the drag force for some particles sizes (125 μ m < d< 600 μ m).

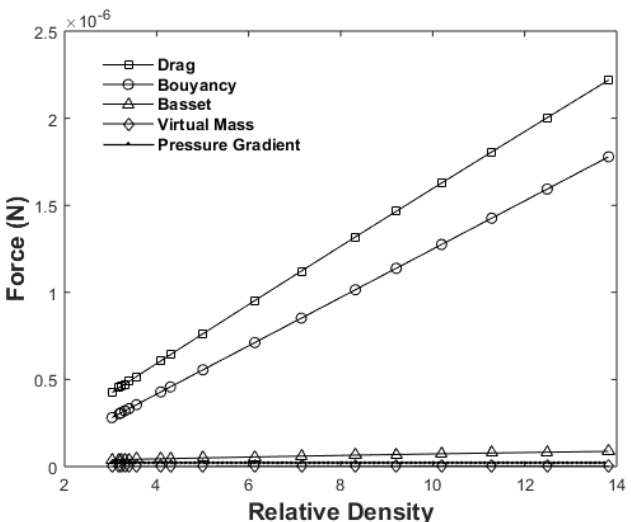


Fig. 3. Relative effect of the different hydrodynamics forces respects to the density, to uniformly sized mineral particles. Source: Authors.

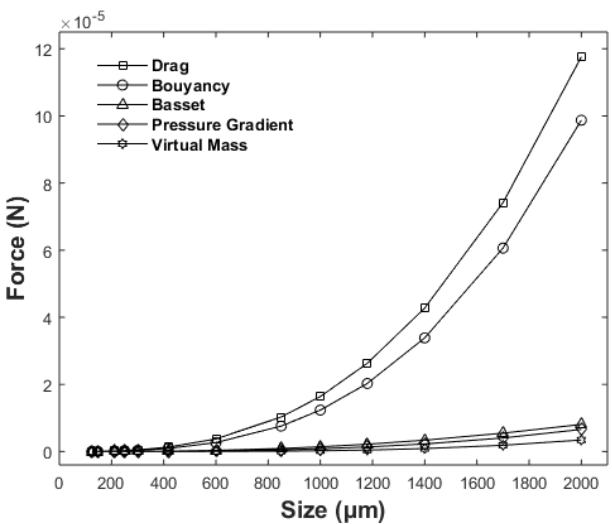


Fig. 4. Relative effect of the different hydrodynamics forces respects to the size, to mineral particles of constant density. Source: Authors.

Comparing Fig. 3 and Fig. 4, the size has a stronger effect on changes of different forces than density does. Overall, Basset force, pressure gradient force and virtual mass force are relative small. But if there is a pulsating flow in the jig, the water flow

accelerating exists, these forces might increase by one or more orders in magnitude as the size and density of particles is increased. In uniform flows where no velocity gradient exists, these forces may be neglected without considerable errors.

Fig. 5 shows that for the density ranges considered in this study, the Basset force is more significant than the virtual mass force and pressure gradient force. Also from Fig. 5 one can see that as the density increases, Basset force and virtual mass force varies exponentially, significantly influencing particle motion and their subsequent concentration.

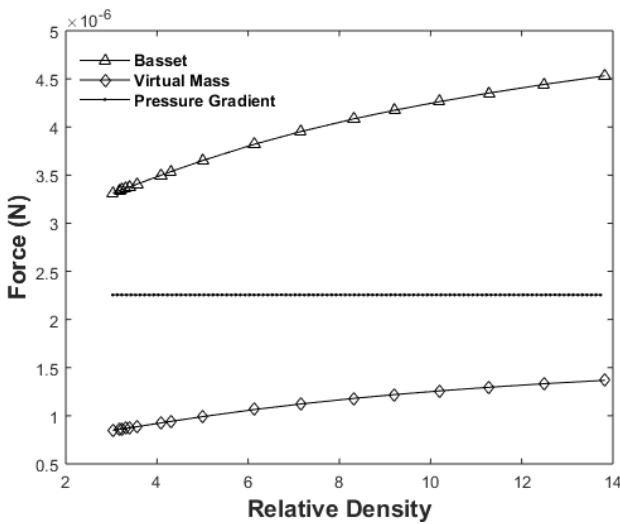


Fig. 5. Comparison of Basset force, virtual mass force and pressure gradient force respect to density. Source: Authors.

5.2. Effect of pulsation addition

In the simulation, the movement of particles can be tracked inside the jig separation chamber, and a visual display of particle stratification can be made. When the particles are fed, stratification happens after few pulsation cycles (4 cycles). Fig. 6 shows the pulsating movement of particles subjected to water flow with sinusoidal pulsation profile. This profile has an amplitude A=5 mm and oscillation period T=0.2 s. These values are chosen since it must be guaranteed that the fluid velocity is greater than the minimum fluidization rate of the artificial porous bed. As the particle motion is pulsating, it is showing the effect of solid-liquid interaction between the phases present in the jig, where the particles oscillate at the same frequency, but its amplitude is proportional to the amplitude of water. The particle motion is strongly affected by density.

As vary the particle density, the lightest particles (ρ <4000 kg/m3) follow an upward movement and heavier particles (ρ >=4000 kg/m3) settle to the

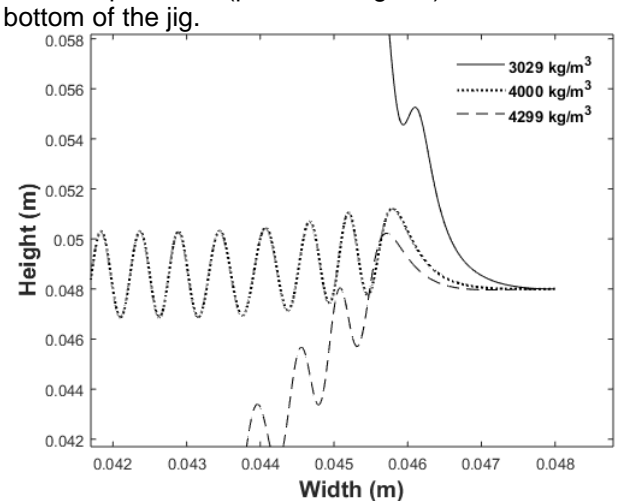


Fig. 6. Particle motion in a sinusoidal pulsation profile with an amplitude of 5 mm and frequency of 5 Hz. Source: Authors.

The rate at which the particles reach their stratification is different, while a light particle takes about t=2 s to leave the column jig, the heavy particles, takes longer time to settler at the bottom.

The above analysis shows the need to study how the particles subjected to different pulsation conditions (amplitude and period) are stratified, this with the aim of optimizing the concentration equipment and thus achieve a good recovery of the mineral particles of interest.

5.3 Inertial forces effect on particles trajectory

From the analysis in section 5.1, the Basset force, virtual mass force and pressure gradient force are found to be significant and should not be ignored when they are used in gravity concentration equipments, where they work with mineral particles suspensions that have wide distributions of density and size.

This section looks the effect forces combinations have in the determining of particle trajectory entering to the jig chamber separation. The parameters that are held constant unless otherwise specified are particle size and initial particle velocity in longitudinal and axial directions. They are d=300 μ m, u_{px} =0.001587 m/s and u_{py} =0 m/s, respectively.

Relative density was evaluated in two values RD = 3.562 and RD = 13.8. The particles were pulsated into a 5 x 10 cm² area injected from a position x=0.048 m and y=0.048 m. A sinusoidal type of waveform was imparted to the water, where the amplitude and frequency of oscillation velocity were set at 0.08816 m/s and 5 Hz, respectively.

The most basic form of the model contains the drag, gravity and pressure gradient forces. The virtual mass force and the Basset history force are successively added to the model. Fig. 7 and Fig. 8 show the results.

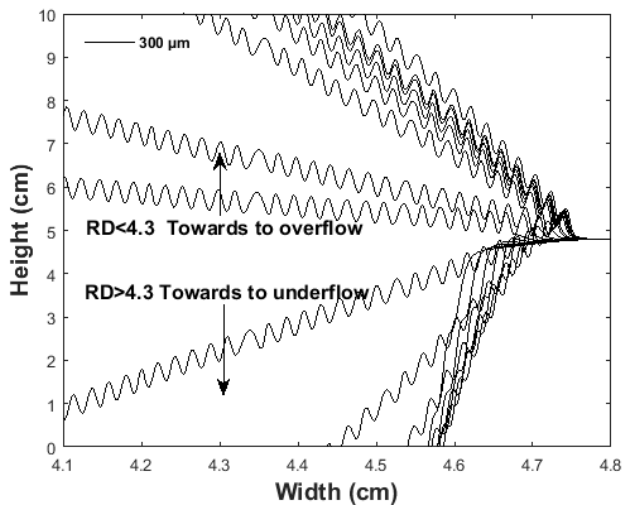


Fig. 7. Particles trajectory by varying the relative density. Source: Authors.

For this case Fig. 7 display the complete trajectories of size uniform particles that varies in a relative density range from 3.026 to 13.8 in the jig. In Fig. 8 (particle of RD=3.562), the Basset force increases the length of trajectory by about ten times particle diameter while the virtual mass force appears to have a slightly lesser effect on the trajectory. The results with the virtual mass force include are consistent with the analysis about a small velocity gradient develops across the particle because of its size. As a result, the virtual mass force has a relatively small effect.

When Basset force is included, particle oscillations amplitude decreases while the longitudinal displacement increases causing that the particle resident time increases inside chamber jig. From Fig. 7 and Fig. 8 is observed that particles with RD ≤ 4.3 will be reported directly in the overflow while

the particles with RD > 4.3 fall to jig bed and will be reported in the concentrate stream.

The hydrodynamic forces acting on the particle trajectory in gravimetric concentration device vary with particle size, particle density and suspension properties.

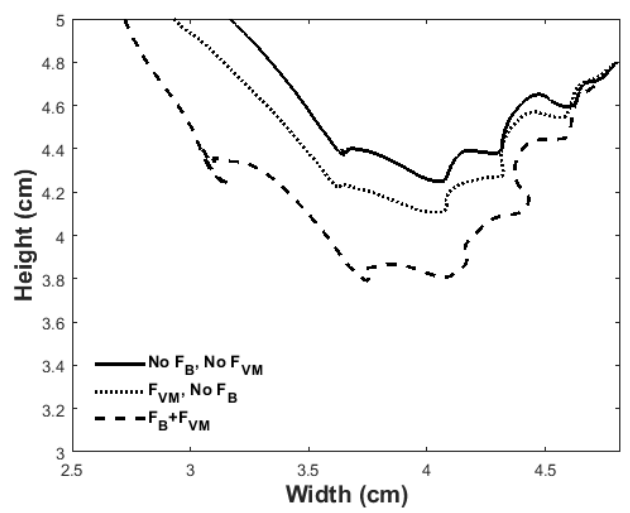


Fig.8. Effect of virtual mass force and Basset force on the particle fine trajectory with relative density of 3.56. Source: Authors.

Virtual mass force and Basset force affect significantly particle trajectories inside the jig chamber. Finally, it could be demonstrated from Fig. 8, that neglect these forces on particle motion model for pulsating beds not generate a good explanation of the phenomenon of solid-liquid interaction in gravimetric concentrations device.

6. CONCLUSIONS

The hindered-settling velocity is a function of particle size, particle density and suspension properties by calculations of isolated heavy particles. Although it was found that the drag force and buoyancy force are dominant forces in determination of particle motion. It was determined in this study that the effect of Basset force, virtual mass force and pressure gradient force on particles trajectories inside the jig bed in a non-uniform pulsating flow are significant, representing particle stratification inside the jig bed a more accurate way.

The stratification of heavy particles in a concentration device type jig has been investigated by the Euler–Lagrangian approach. The model also

simulates the time-dependent, two-dimensional motion of minerals particles in water with wide size and density distributions. The model incorporates relevant hydrodynamics forces acting on a particle in a liquid. The liquid phase hydrodynamics is described using Unsteady Reynolds averaged Navier-Stokes equations (URANS).

The study of the transient motion of particles developed in this work has provided a better understanding of particle stratification in gravimetric concentration devices using oscillating flows. As discussed previously, the transport mechanisms brought up to the model by the inertial forces are of major importance in the description of particle trajectories whose inertia is comparable to the inertia of the fluid. In particulate systems in which the inertia of the fluid is considerably smaller than the inertia of the particles (as typically occurs in gas-solid suspensions), the inertial forces can be neglected with no relevant consequences to a correct prediction of the dynamics of these systems. However, the derivation of a model for pulsating flows considering such effects (drag, buoyancy and inertial forces) is still an open problem and needs further numerical and experimental research that helps to improve equipment performance as gravitational concentrator.

The qualitative results indicate that a study involving the interaction between particles (particle-particle interaction forces or so-called solid-solid contact forces) is necessary for a more detailed understanding of the operation of the concentrator equipment. However, the research demonstrates the usefulness of the Eulerian-Lagrangian model, as an effective numerical model to study the concentration process. It requires additional work that considers different amplitudes and periods of pulsation as in Ospina*et al* [22], in addition to a quantitative analysis that helps to understand and optimize the performance of the device through the physical principles of conservation than describe it.

7. ACKNOWLEDGMENTS

The authors would like to thank at the Instituto Tecnológico Metropolitano and Banco de la República for financing the research project. Agreement 201629.

8. REFERENCES

- [1] M. O. Bustamante, A. C. Gaviria, and O. J. Restrepo, Class notes of the subject: minerals Concentration. Medellín: Universidad nacional de Colombia-sede Medellín. 2008.
- [2] R. O. Burt, "The role of gravity concentration in modern processing plants," *Miner. Eng.*, vol. 12, no. 11, pp. 1291–1300, Nov. 1999.
- [3] S. Cierpisz, "A dynamic model of coal products discharge in a jig," *Miner. Eng.*, vol. 105, pp. 1–6, 2017.
- [4] T. Phengsaart, M. Ito, N. Hamaya, and C. Baltazar, "Improvement of jig efficiency by shape separation, and a novel method to estimate the separation efficiency of metal wires in crushed electronic wastes using bending behavior and 'entanglement factor," *Miner. Eng.*, vol. 129, no. May, pp. 54–62, 2018.
- [5] F. Pita and A. Castilho, "Influence of shape and size of the particles on jigging separation of plastics mixture," *Waste Manag.*, vol. 48, pp. 89–94, 2016.
- [6] R. O. Burt, Gravity concentration technology, Vol 5. Amsterdam, Netherlands: Elsevier, 1984.
- [7] M. A. A. Aziz, K. M. Isa, N. J. Miles, and R. A. Rashid, "Pneumatic jig: effect of airflow, time and pulse rates on solid particle separation," *Int. J. Environ. Sci. Technol.*, no. January, pp. 1–12, 2018.
- [8] K. J. Dong, S. B. Kuang, a. Vince, T. Hughes, and a. B. Yu, "Numerical simulation of the in-line pressure jig unit in coal preparation," *Miner. Eng.*, vol. 23, no. 4, pp. 301–312, Mar. 2010.
- [9] S. M. Viduka, Y. Q. Feng, K. Hapgood, and M. P. Schwarz, "Discrete particle simulation of solid separation in a jigging device," *Int. J. Miner. Process.*, vol. 123, pp. 108–119, Sep. 2013.
- [10] F. W. Mayer, "Fundamentals of a potential theory of jigging process," in 7th International Minerals Processing Congress,

1964, pp. 75-86.

- [11] L. M. Tavares and R. P. King, "A Useful Model for the Calculation of the Performance of Batch and Continuous Jigs," *Coal Prep.*, vol. 15, no. 3–4, pp. 99–128, 1995.
- [12] Y. Xia, F. F. Peng, and E. Wolfe, "CFD simulation of fine coal segregation and stratification in jigs," *Int. J. Miner. Process.*, vol. 82, no. 3, pp. 164–176, 2007.
- [13] Y. K. Xia and F. F. Peng, "Numerical simulation of behavior of fine coal in oscillating flows," *Miner. Eng.*, vol. 20, no. 2, pp. 113–123, 2007.
- [14] S. Viduka, Y. Feng, K. Hapgood, and P. Schwarz, "CFD-DEM investigation of particle separations using a Trapezoidal jigging profile," in *Ninth International Conference on CFD in the Minerals and Process Industries*, 2012, pp. 1–8.
- [15] S. Viduka, Y. Feng, K. Hapgood, and P. Schwarz, "CFD-DEM investigation of particle separations using a sinusoidal jigging profile," *Adv. Powder Technol.*, vol. 24, no. 2, pp. 473–481, 2013.
- [16] R. Srinivasan, B. K. Mishra, and S. P. Mehrotra, "Simulation of Particle Stratification in Jigs Simulation of Particle Stratification in Jigs," *Coal Prep.*, vol. 20, no. 1–2, pp. 55–70, 1999.
- [17] B. K. Mishra and S. P. Mehrotra, "Modelling of particle stratification in jigs by the discrete element method," *Miner. Eng.*, vol. 11, no. 6, pp. 511–522, 1998.
- [18] B. K. Mishra and S. P. Mehrotra, "A jig model based on the discrete element method and its experimental validation," *Int. J. Miner. Process.*, vol. 63, pp. 177–189, 2001.
- [19] A. J. . Beck and P. N. Holtham, "Computer simulation of particle stratification in a two-dimensional batch jig," *Miner. Eng.*, vol. 6, no. 5, pp. 523–532, 1993.
- [20] M. A. Ospina-Alarcón and M. O. Bustamante-Rúa, "Hydrodynamic study of

- gravity concentration devices type JIG," *Rev. Prospect.*, vol. 13, no. 1, pp. 52–58, 2015.
- [21] M. A. Ospina-Alarcón, "Modelamiento de la hidrodinámica de la separación gravimétrica de minerales en jigs," Universidad Nacional de Colombia, 2014.
- [22] M. A. Ospina-Alarcón, A. B. Barrientos-Ríos, and M. O. Bustamante-Rúa, "Influence of the pulse wave in the stratification of high density particles in a JIG device," Rev. TecnoLógicas, vol. 19, no. 36, pp. 13–25, 2016.
- [23] E. F. Crespo, "Modeling segregation and dispersion in jigging beds in terms of the bed porosity distribution," *Miner. Eng.*, vol. 85, pp. 38–48, 2016.
- [24] K. Asakura, M. Nagao, and M. Mizuno, "Simulation of Particle Motion in a Jig Separator," *J. JSEM*, vol. 7, no. Special Issue, 2007.
- [25] K. Asakura, S. Harada, T. Funayama, and I. Nakajima, "Simulation of descending particles in water by the distinct element method," *Powder Technol.*, vol. 94, pp. 195– 200, 1997.
- [26] B. Mohammadi and O. Pironneau, *Analysis* of the k-epsilon turbulence model. New York: Jonh Wiley & Sons, 1994.
- [27] K. Asakura, M. Mizuno, M. Nagao, and S. Harada, "Numerical Simulation of Particle Motion in a Jig Separator," in 5th Join ASME JSME Fluids Engineering Conference, 2007, pp. 385–391.
- [28] G. Rudinger, "Fundamentals of Gas-Particle Flow," in *Handbook of Powder Technology*, vol. 2, Amsterdam, Netherlands: Elsevier, 1980, pp. 1–142.
- [29] M. Sommerfeld and N. Huber, "Experimental analysis of modelling of particle-wall collisions," *Int. J. Multiph. Flow*, vol. 25, no. 6–7, pp. 1457–1489, 1999.

- [30] Y. D. Sobral, T. F. Oliveira, and F. R. Cunha, "On the unsteady forces during the motion of a sedimenting particle," *Powder Technol.*, vol. 178, no. 2, pp. 129–141, 2007.
- [31] S. V. Patankar, *Numerical Heat Transfer and Fluid Flow.* New York: Hemisphere Publishing Corporation, 1980.
- [32] H. P. Zhu, Z. Y. Zhou, R. Y. Yang, and A. B. Yu, "Discrete particle simulation of particulate systems: A review of major applications and findings," *Chem. Eng. Sci.*, vol. 63, no. 23, pp. 5728–5770, 2008.
- [33] A. B. Basset, A Treatise on Hidrodynamics, Volumen II. London, UK: George Bell and Sons, 1988.
- [34] L. Schiller and A. Naumann, "Über die grundlegenden Berechnungen bei der Schwerkraftaufbereitung," Ver. Deut. Ing., vol. 77, pp. 318–320, 1933.
- [35] H. K. Versteeg and W. Malalasekera, An Introduction to Computational Fluid Dynamics., 2nd ed. London, UK: Pearson Education, 2007.
- [36] S. V. Patankar and D. B. Spalding, "A calculation procedure for heat, mass and momentum transfer in three-dimensional parabolic flows," *Int. J. Heat Mass Transf.*, vol. 15, no. 10, pp. 1787–1806, 1972.
- [37] C. Coimbra and R. Rangel, "General solution of the particle momentum equation in unsteady Stokes flows," *J. Fluid Mech.*, vol. 370, pp. 53–72, 1998.
- [38] G. K. Batchelor, *An Introduction to Fluid Dynamics*. Cambridge, UK: Cambridge University Press, 1967.
- [39] H. Lamb, *Hydrodynamics*, 6th ed. New York: Cambridge University Press, 1975.
- [40] L. M. Milne-Thomson, *Theoretical Hydrodynamics*, 5th ed. London, UK: Macmillan & Co Ltd, 1962.